

No. 123/22, 7–17
ISSN 2657-6988 (online)
ISSN 2657-5841 (printed)
DOI: 10.26408/123.01

Submitted: 08.12.2021
Accepted: 07.02.2022
Published: 30.09.2022

BAND K SATELLITE RECEIVER SIGNAL AND RADIO LOCATOR

Marian Wnuk

Military University of Technology, 00-908 Warszawa, ul. Gen. Sylwestra Kaliskiego 2,
Poland, Faculty of Electronics, e-mail: marian.wnuk@wat.edu.pl,
ORCID 0000-0003-4576-4023

Abstract: The last dozen or so years has seen significant and dynamic development in satellite technologies. Devices using satellites circulating in space for the purposes of general communication have ceased to be the domain of a narrow group of recipients (mainly increased use by the military, governments and the media) and instead gained increasing numbers of new users. The paper presents a developed station for receiving satellite signals in the K band, with particular emphasis on the design and alignment of the antenna in the Cassegrain system.

Keywords: automatic control, design automation receiving antennas, reflector antennas.

1. INTRODUCTION

In recent years we have observed the huge and dynamic growth in satellite technologies. Equipment that uses satellites circulating in space for communication are no longer available to a limited group of users (mainly the military, governments and the media). Satellite communication has begun to be used by a wider group of users.

The main factors allowing the dynamic use of satellite communication [Berioli, Courville and Werner 2007] has been:

- enhanced satellite technologies, for better network reliability and speed;
- decreased price of equipment and available services.

Satellite communication is defined as a type of radio communication with global coverage, using retransmitting satellites as stations mediating in maintaining communication between cooperating stations on earth [Dunlop, Girma and Irvine 2000]. Satellite communications between an Earth base station and a special object involves the transmission of information in both directions, where the amount of information depends on the direction it is sent. The technical and use requirements for satellite systems are: wide flexibility in the use of satellite channels; high quality and reliability in communications; higher frequency ranges; and antennas with a controlled radiating bundle.

At the peak in the development of satellite telecommunication, geostationary satellites were almost always used; however, they have a number of disadvantages, such as high absorption and the significant delay in the signal via Earth-satellite and satellite-Earth routes. One solution is to use a satellite located on an elongated elliptic orbit (with a maximal height of around 40000 km over the northern hemisphere). Satellites located on elongated elliptic orbits have similar characteristics (good and bad) to geostationary satellites, with the exception of stationarity orbits (an observer on Earth's surface sees only a slow movement of the satellite) [Boussemart, Berioli and Fondere 2007]. In telecommunication practice, two different types of these systems exist: low orbit LEO systems, numbering at least a dozen, of moving versus Earth satellites, placed on many circular orbits, to enable the global range of the system along with high orbit geostationary GEO systems with a couple of stationary satellites located on one equator orbit, which are unable to cover the polar areas [Mohamed 2013]. The disadvantage of low orbit systems is the very high cost of their telecommunication infrastructure, due mainly to the high number of satellites. However, with low located satellites these systems are best in terms of propagation delays in the radio signal, which enables the provision of multimedia services [Ghasemi, Abedi and Ghasemi 2011]. However, high orbit systems are characterized by reverse characteristics, which means that the cost of the telecommunication infrastructure is relatively low, while the high propagation delays mean that they see limited use in advanced telecommunication services [Berioli, Courville and Werner 2007; Joseph 2012]. This is why stations, to receive signals, need to work in defined frequency ranges, require high-sensitivity receiving systems and the ability to track the trajectory of a satellite. Satellites moving in a low orbit take about 90 minutes to move around the Earth. Placing a satellite in a low Earth orbit requires lower power transmitters to achieve transmission [Bem and Zieliński 2000], and therefore this part of space is also used for communication purposes, especially in frequency bands where there is low signal attenuation, such as in the K band [Bayer et al. 2016]. The second condition for receiving signals from a satellite moving in a low orbit is the need to use tracking systems, which means the antennas of these systems are in constant motion. This applies to satellites used in military communication systems.

2. CONSTRUCTION OF THE STATION

The diagram of the system for receiving and locating the signals in the K band is shown in Figure 1 [Dybdal 2009; Hein et al. 2010].

It consists of three basic blocks:

1. Receiving the microwave path, consisting of a Cassegrain antenna system connected to a highly sensitive receiver for the frequency conversion.
2. Microprocessor system for controlling the position of the antenna and reading the coordinates of the radiation source.

3. Antenna column with drive and power supply systems.

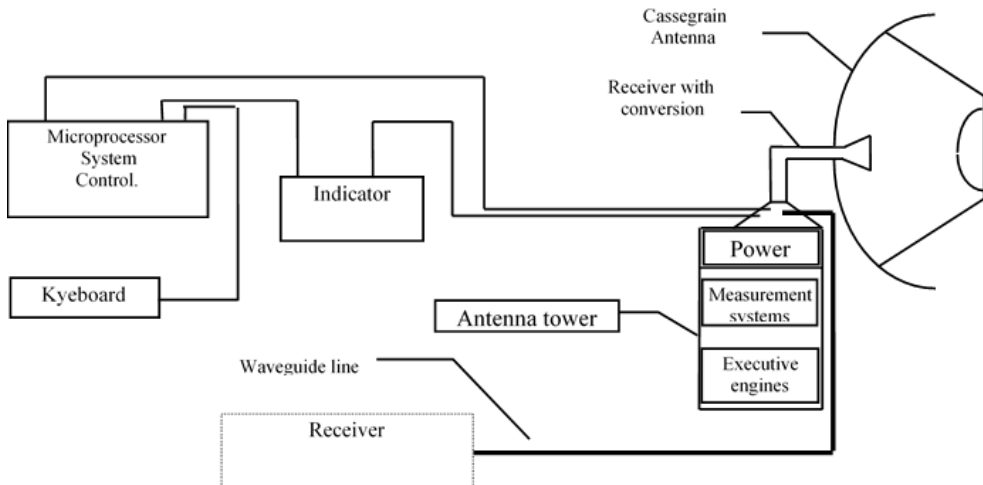


Fig. 1. Device for receiving and locating satellite signals

In order to ensure the reception of low-level signals, the antenna must have a high directional gain, which can be provided by a dual-reflector antenna. When designing reflector antennas, the principles of geometric optics are widely used:

- principle of the conservation of energy in elementary sections;
- law of equality of incidence and reflection angles (on the reflector and the counter-reflector);
- additionally, it also uses the conditions resulting from antenna structure geometry;
- collinearity of the rays reflected from the reflector;
- condition of the synphase of the field in the aperture (the same path length for all rays from the phase center of the tube to the reflector aperture).

Due to the constantly growing requirements for low-level side lobes in the radiation pattern, the phenomenon of wave diffraction at the edge of the reflector and the counter-reflector can be increasingly taken into account. Geometric optics is not enough in this case, and the computational methods of the geometric theory of diffraction should be used [Balanis 2005; Winterstein and Greda 2017].

The radiation pattern, $G(\theta)$, of the Cassegrain antenna in Figure 2 can be presented as the radiation pattern of a circular aperture (diameter D) with a notch in the center (a counter-reflector with diameter d) and the influence of mounting the counter-reflector with a circular aperture and symmetrical field distribution in the aperture, $E(\rho)$, taken into account. In our case, the diameter of the parabolic antenna

is 3 m. The radiation pattern is calculated using the formula [Boussemart, Berioli and Fondere 2007]:

$$G(\Theta) = \int_0^1 r f(r) J_0(u, r) dr - \eta^2 \int_0^1 r f(r) J_0(u, \eta, r) dr \quad (1)$$

where:

$$u = (\pi/\lambda) D \sin(\theta),$$

D – aperture diameter,

λ – wavelength,

F – spotlight focal length,

r – current, normalized to the radius of the reflector (0.5 D), the aperture radius,

$J_0(u, \eta, r)$ – Bessel function.

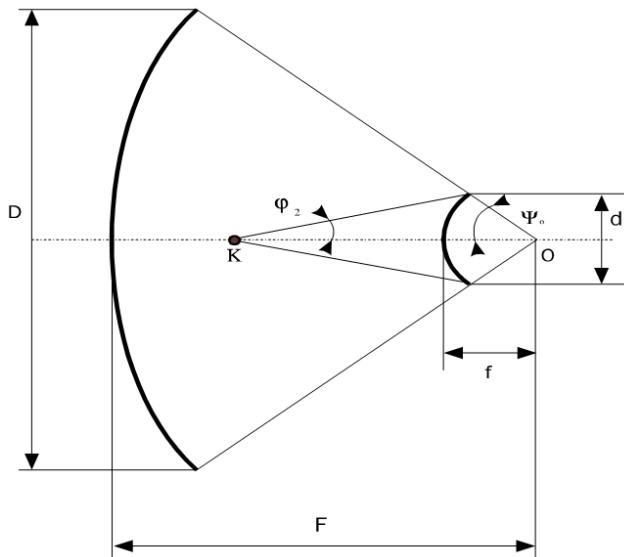


Fig. 2. Cassegrain antenna

The shape of the radiation pattern, $G(\theta)$, thus depends only (after introducing the normalizing parameter, u) on the field distribution, $E(\rho)$. This is very important in the practice of antenna design, as it allows the calculations to use the $E(\rho)$ field distribution instead of the $G(\theta)$ radiation pattern.

The field distribution in the Cassegrain symmetrical antenna aperture is expressed by the following formula [Warren 2013]:

$$E(\rho) = F(\varphi(\rho)) \left\{ \frac{\sin[\varphi(\rho)]}{\sin[\psi(\rho)]} \right\} \cos^2(0.5\psi(\rho)) \quad (2)$$

where:

$$\sin[\varphi(\rho)] = \sin[0.5(\psi_0 + \varphi_2)] \quad (3)$$

$$\varphi(\rho) = \varphi \left\{ 2 \operatorname{arctg} \left(\frac{e-1}{e+1} \right) \operatorname{tg} \left[\operatorname{arctg} \left(\frac{\rho}{2F} \right) \right] \right\} \quad (4)$$

e – eccentricity of the auxiliary headlamp:

$$e = \frac{\sin[0.5(\psi_0 + \varphi_2)]}{\sin[0.5(\psi_0 - \varphi_2)]} \quad (5)$$

ψ_0 – angle of illumination of the edge of the reflector from the focus of the parabola:

$$\psi_0 = 2 \operatorname{arctg} \left(\frac{D}{4F} \right) \quad (6)$$

In analysing formula 2, it can be observed that the course of the field distribution function on the aperture, $E(\rho)$, is determined by two factors:

1. Radiation pattern of the tube illuminating the counter-reflector, $F(\varphi)$.
2. Antenna geometry [two components – quotient $\sin(\varphi)/\sin(\psi)$ and the length of the path from the focus of the parabola to its surface – $\cos^2(0.5\psi)$].

An important practical conclusion can thus be drawn – the optimization of a dual reflector antenna can be performed in two ways:

1. Choosing a radiation pattern of the lamp, $F(\theta)$, to obtain a given field distribution in the aperture, $E(\rho)$.
2. Selecting the antenna geometry in such a way (specifically the function of the aperture radius, $\rho = \rho(\varphi)$ [Janczak and Marczyk 2009; Winterstein and Greda 2017; Guidotti et al. 2019]) so as to obtain the effect as in point 1.

The $\rho = \rho(\varphi)$ function shows at which point of the aperture, described ρ , the beam sent from the illuminating source at the angle should hit to form the distribution, $E(\rho)$, on the aperture.

By choosing the first method, the radiation pattern of the tube is calculated as the radiation of a rectangular surface with dimensions equal to the outlet of the tube, excited in phase, with a uniform field distribution in the E plane and a cosine wave distribution in the H plane [Elliott 2003]. This more accurate model takes into account the phase shifts appearing in the aperture of the tube.

The following dependencies are then obtained:

- E plane:

$$\phi_E = \frac{\pi}{4} \frac{B^2}{\lambda R_E} \quad (7)$$

$$G_E(\phi) = \int_{-\frac{B}{2}}^{\frac{B}{2}} \int_{-\frac{A}{2}}^{\frac{A}{2}} \exp[ikx \sin(\phi)] + i4 \frac{\phi_E}{A^2} x^2 dx dy \quad (8)$$

- H plane:

$$\phi_H = \frac{\pi}{4} \frac{A^2}{\lambda R_H} \tag{9}$$

$$G_H(\phi) = \int_{-\frac{B}{2}}^{\frac{B}{2}} \int_{-\frac{A}{2}}^{\frac{A}{2}} \exp[iky \sin(\phi)] + i4 \frac{\phi_H}{A^2} y^2 dx dy \tag{10}$$

The characteristics of the horn antenna designed and manufactured on the basis of the above relationships, with rotating polarization, are shown in Figure 3.

The measured directional gain of the manufactured Cassegrain antenna was -53 dB, and the beam width in both planes was less than 20 degrees.

The received signal with left or right circular polarization and the frequency from the K band [Kestilä and Vankka 2013], after amplification, undergoes a linear transformation (using a local heterodyne characterized by high stability of 10^{-8} at a frequency of 10.6 GHz) into a signal with a frequency in the X band, without distortion [Janczak and Marczyk 2009; Guidotti et al. 2019]. After conversion, the signal is sent via a waveguide to the receiver operating in the X band, where it is further processed. The azimuth uses a rotary joint and a low-loss flexible cable in the facade.

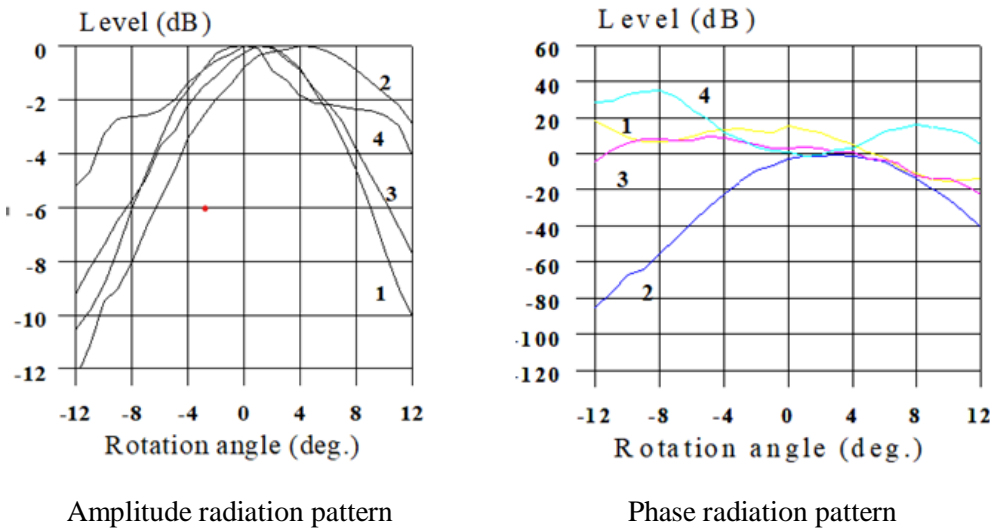


Fig. 3. Feed horn radiation pattern: 1 – vertical polarization at azimuth, 2 – horizontal polarization at azimuth, 3 – vertical polarization in elevation, 4 – horizontal polarization in elevation

The comparison of the theoretical analysis and measurements of the antenna made is shown in Figure 4.

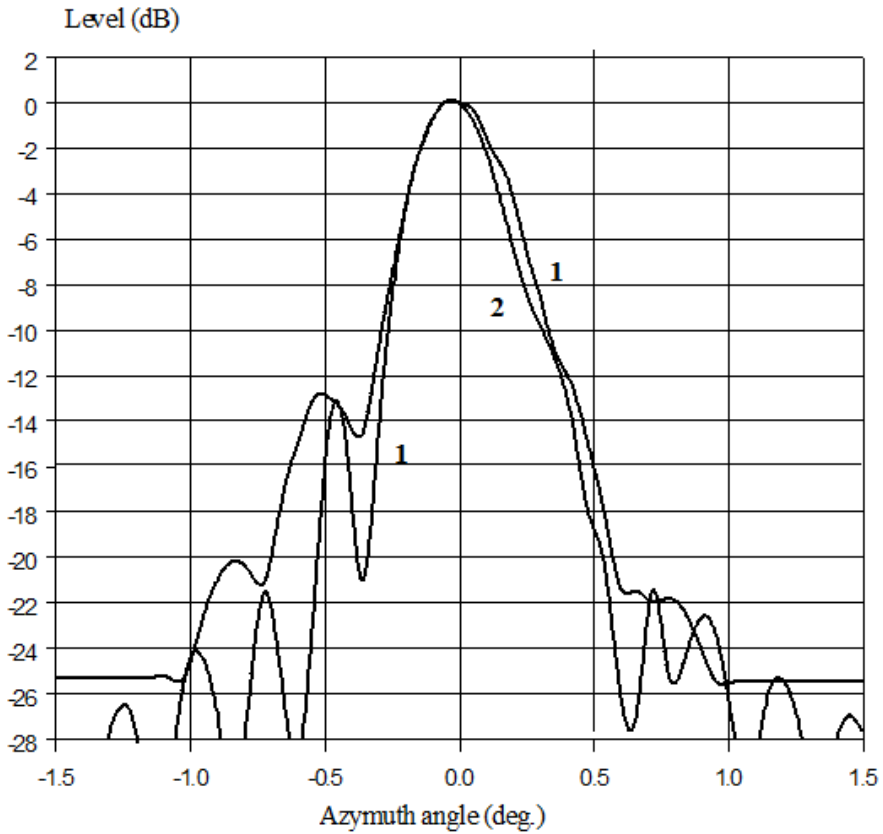


Fig. 4. Radiation pattern for the antenna: 1 – theoretical, 2 – measured

For such a receiver, sensitivity is defined as the ratio of the signal power to the sum of the signal power:

$$S = 10\log(k \cdot T_o) + 10\log(BW) + 10\log(SNR) + \alpha + F_o \quad (11)$$

where:

- $k = 1.38 \cdot 10^{-27} \text{ J/K}$ – Boltzman's constant,
- T_o – antenna temperature,
- BW – frequency response [dB],
- α – attenuation of the track before the amplifier [dB],
- F_o – noise value of the amplifier [dB].

Assuming the frequency response, $BW = 1 \text{ MHz}$, and the signal-to-noise ratio, $SNR = 1$, the relation (1) can be simplified to the form

$$S = 174[\text{dBm}] + 60[\text{dB}] + \alpha + F_o \quad (12)$$

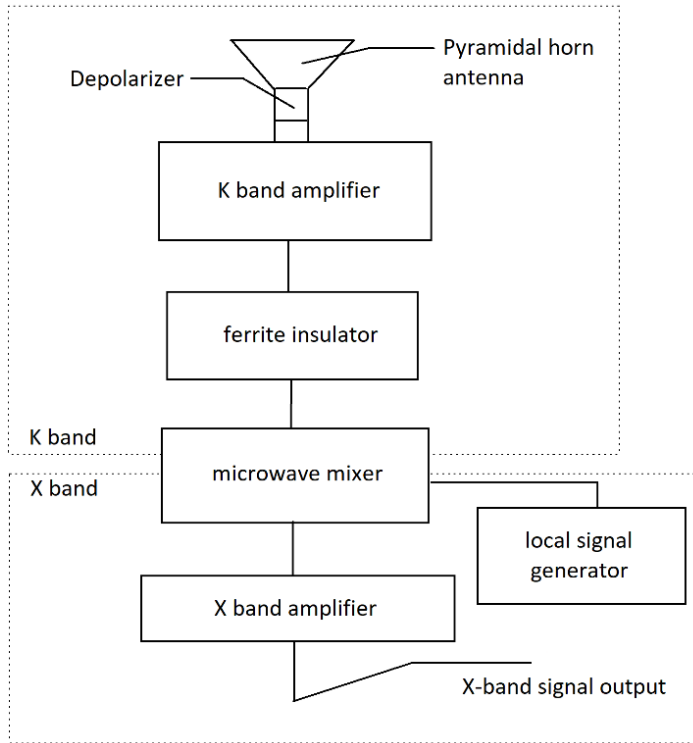


Fig. 5. Block diagram of a microwave receiver

It follows that, in order to determine the sensitivity, it is necessary to determine the losses caused by the circuit preceding the amplifier and the noise figure at the input of the microwave path.

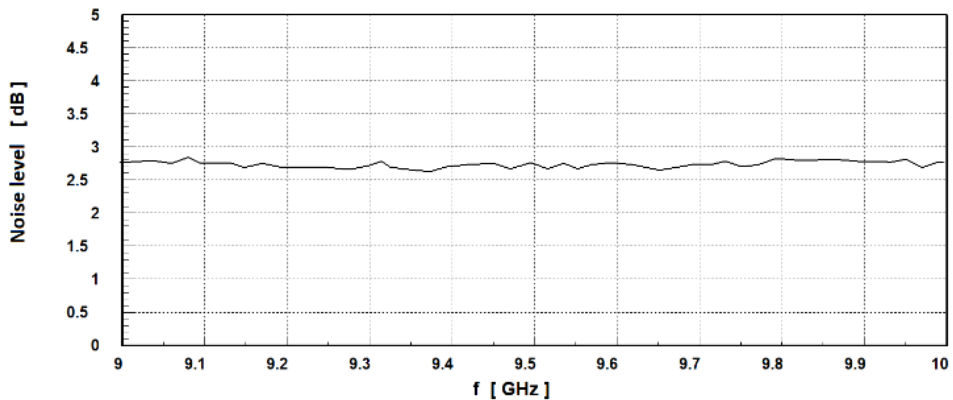


Fig. 6. Noise level output of the circuit

The measured gain of the circuit is 54.9 dB. By taking into account the antenna gain, the sensitivity of the microwave system is 10^{-14} W.

4. MICROPROCESSOR CONTROL SYSTEM

The antenna is mounted on the antenna column, which enables its rotation in the horizontal plane (azimuth) in the range from 0 to 360 degrees and in the vertical plane (elevation) in the range from -1 to +90 degrees. The column is equipped with two drive systems, consisting of backlash-free gears driven by DC motors [Aung and Ya 2015].

The antenna position control system is based on a microprocessor, see Figure 7.

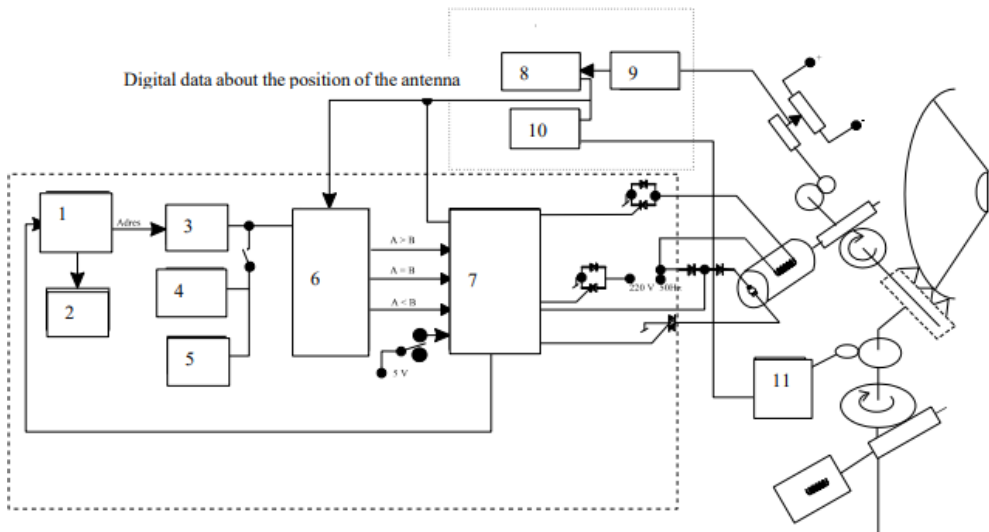


Fig. 7. Block diagram of the microprocessor control system

1. Programmer; 2. Step indicator address; 3. Memory chip; 4. Elevation data; 5. Azimuth data; 6. Comparator; 7. Automation control system; 8. Elevation indicator; 9. Azimuth indicator; 10. A/C converter. The measurement of the current position of the antenna in the facade is made with a resistance converter (multi-turn potentiometer). The resistance value is changed to voltage, which is then processed in the A/D converter and displayed on the gauge

To measure the position of the antenna at the azimuth, an impulse transducer was used [Drieß, Evers and Brückner 2012; Liping 2017]. The position of the antenna at azimuth is converted into an appropriate number of pulses, which after conversion to the value of the angle is displayed on the indicator. Current data from the transducers are fed to the B inputs of the comparator. The given coordinates of the antenna position from the memory are entered into the A input of the comparator.

The comparator generates an error signal, which is fed to the automation systems that control the operation of the motors (excitation windings). After equalizing the signals fed to the A and B inputs of the comparator, the automatic systems give the STOP command and the motors stop. Approaching the given coordinates takes place by the shortest path and with the maximum speed of the motors. When approaching a position different by $\pm 1.0^\circ$, the motors slow down and move to the set position.

5. CONCLUSIONS

The LEO station for receiving satellite signals from satellites located in low-lying orbits presented in the article fulfilled the tasks set for it. The applied lighting system of the Cassegrain antenna, with a useful beam width below 20 degrees and a directional gain, should be approx. 53 dB to allow the reception of signals of any polarization. It is characterized by high sensitivity in the order of 10^{-14} W, partly due to the use of an antenna in the Cassegrain system as well as a highly sensitive amplifier with a low noise level. This allows it to follow the movement of the selected satellite by programming the receiver to receive the maximum signal. It ensures reception of signals across the full azimuth range, i.e. 360° , and in elevation by $\pm 90^\circ$. The station is designed to receive satellite signals in the second propagation of the 22 GHz band.

REFERENCES

- Aung, N.W, Ya, A.Z., 2015, *Microcontroller Based Electrical Parameter Monitoring System of Electronic Load Controller Used in Micro Hydro Power Plant*, Journal of Electrical and Electronic Engineering, vol. 3, no 5, pp. 97–109.
- Balanis, C.A., 2005, *Antenna Theory and Design*, John Wiley & Sons, Inc.
- Bayer, H., Krauss A., Zaiczek T., Stephan R., Enge-Rosenblatt O., Hein, M.A., 2016, *Ka-Band User Terminal Antennas for Satellite Communications*, IEEE Antennas & Propagation Magazine.
- Bem, D.J., Zieliński R.J., 2000, *Satellite Access Systems*, Przegląd Telekomunikacyjny i Wiadomości Telekomunikacyjne, pp. 593–601.
- Berioli, M., Courville N., Werner M., 2007, *Emergency Communications over Satellite: the WISECOM Approach*, 16th IST Mobile and Wireless Communications Summit, Hungary, July 1–5, pp. 1–5.
- Berioli, M., Courville N., Werner M., 2007, *Integrating Satellite and Terrestrial Technologies for Emergency Communications: the WISECOM Project*, Qshine: International Conference on Heterogeneous Networking for Quality, Reliability, Security and Robustness, Vancouver, British Columbia, August 14–17.
- Boussemart, V., Berioli M., Fondere J.L., 2007, *TETRA over DVB-RCS for Emergency Communications*, Conference: Proceedings of the 12th WSEAS International Conference on Communications.

- Drieß, P., Evers F., Brückner M., 2012, *A Resource Management Architecture for Mobile Satellite-based Communication Systems*, Proc. Eighth Advanced International Conference Telecommunications, Stuttgart, pp. 138–143.
- Dunlop, J., Girma D., Irvine J., 2000, *Digital Mobile Communications and the TETRA System*, John Wiley & Sons, Ltd., Chichester, England.
- Dybdal, R., 2009, *Communication Satellite Antennas: System Architecture, Technology, and Evaluation*, The McGraw-Hill Companies.
- Elliott, R.S., 2003, *Antenna Theory and Design*, John Wiley & Sons, Inc.
- Ghasemi, A., Abedi, A., Ghasemi F., 2011, *Propagation Engineering in Wireless Communications* Springer Science+Business Media, LLC.
- Guidotti, A., Vanelli-Coralli, A., Foggi, T., Colavolpe, G., Caus, M., Bas, J., Cioni, S., Modenini, A., 2019, *LTE-based Satellite Communications in LEO Mega-Constellations*, International Journal of Satellite Communications and Networking, vol. 33, pp. 316–330.
- Hein M.A., Bayer, H., Krauss, A., Stephan, R., Volmer, C., Heuberger, A., Eberlein, E., Keip, C., Mehnert, M., Mitschele-Thiel, A., Driess, P., Volkert, T., 2010, *Perspectives for Mobile Satellite Communications in Ka-band (MoSaKa)*, Proc. 4th European Conference Antennas Propagation, Barcelona, Spain, pp. 1–5.
- Janczak, J., Marczyk, M., 2009, *The Use of Satellite Communication in Multinational Operations*, AON, Warszawa.
- Joseph L., 2012, *Awange Environmental Monitoring Using GNSS Global Navigation Satellite Systems*, Springer, Berlin, Germany.
- Kestilä, A., Vankka, J., 2013, *Sun Outage Calculator for Satellite Communications*, IEEE International Conference on Space Science and Communication, Melaka, Malaysia, pp. 51–56.
- Kolawole, M.O., 2002, *Satellite Communication Engineering*, CRC Press, Boca Raton, FL, USA.
- Liping, A., 2017, *Ka-band HTS Channel Uplink SNIR Probability Model*, vol. 36, no. 1, pp. 146–164.
- Mohamed, A., 2013, *Global Navigation Satellite Systems –from Stellar to Satellite Navigation*, InTech Janeza Trdine 9, 51000 Rijeka, Croatia.
- Stutzman, W.L., Thiele, G.A., 2013, *Antenna Theory and Design*, John Wiley & Sons, Inc.
- Winterstein, A., Greda, Ł.A., 2017, *An Adaptive Calibration and Beamforming Technique for a GEO Satellite Data Relay*, International Journal of Satellite Communications and Networking, vol. 36, no. 2, pp. 207–219.